ISSN 2622-9374 (Online)

Asian Institute of Research

# Engineering and Technology Quarterly Reviews

Vol. 5, No.1 June 2022

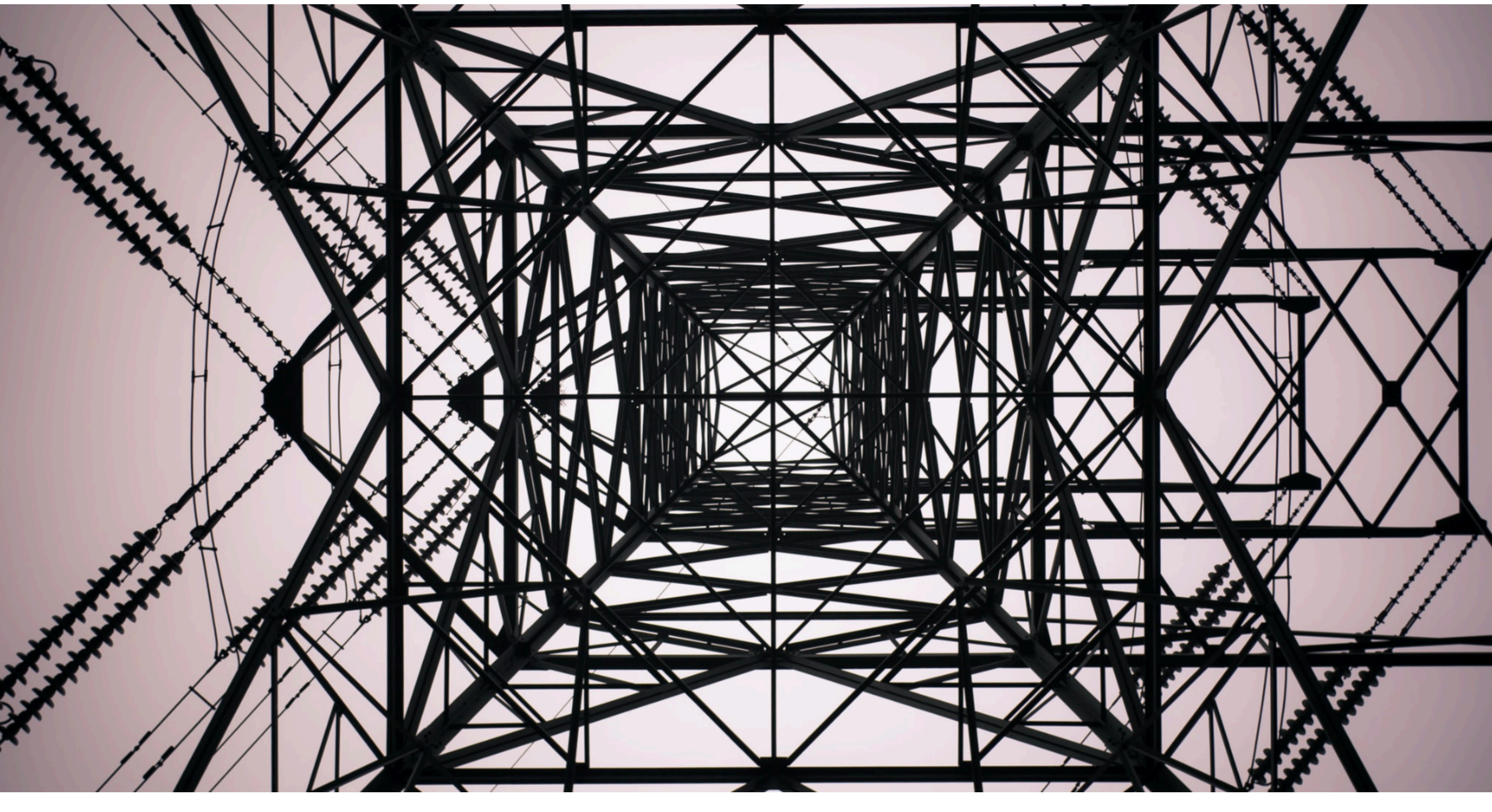

Asian Institute of Research
Connecting Scholars Worldwide

Asian Institute of Research
**Engineering and Technology Quarterly Reviews**
Vol.5, No.1 June 2022

Engineering and Technology
Quarterly Reviews
ISSN 2622-9374 (Online)

ISSN 2622-9374 (Online)

ASIAN INSTITUTE OF RESEARCH
Connecting Scholars Worldwide

The Asian Institute of Research
Engineering and Technology Quarterly Reviews
Vol.5, No.1, 2022: 1-8
ISSN 2622-9374


# Design of Land Selection Model for Sustainable Rice Field Direction Using SIG Technology in Kurik District of Merauke of Papua

Susanto[1], Irene Ike Praptiwi[2]

[1] Teknik Informatika Department, Teknik Faculty UNMUS Merauke. Email: Susanto@unmus.ac.id
[2] Peternakan Department, Pertanian Faculty UNMUS Merauke, Papua, Indonesia. Email: irineike@gmail.com

**Abstract**
Kurik District is a rice production center in Merauke Regency. The use of rice field agricultural land in Kurik District needs to be optimized for improving community welfare and the road to national food sovereignty. Until now Kurik District has not established the existence of sustainable rice fields in order to maintain food security. Determination of sustainable rice fields must be adjusted to the actual conditions of rice fields, such as water availability conditions, land intensity and rice productivity. In determining sustainable rice fields can be identified using the help of remote sensing imagery. This study aims to 1) review the ability of Landsat 8 image for interpretation of rice farming intensity based on the planting calendar 2) to find out the distribution of sustainable rice fields based on actual land criteria. Sustainable rice fields are determined by using matching methods against established criteria. The criteria that have been set consist of interrelated parameters, such as water availability, field intensity, and rice productivity. In determining the direction of sustainable rice fields first, a visual interpretation of the image of the sharpening image fussion to find out the condition of water availability, the intensity of the land with multitemporal imagery based on the planting calendar, and landform units. The results of this study have been made a model of sustainable rice field selection in Kurik District of Merauke Regency Papua.

**Keywords:** Sustainable Rice Fields, Rice Productivity, SIG, Kurik District

## 1. Introduction

Merauke Regency is the largest district in Papua Province and in Indonesia which is 46,791.63 km2 The vast natural potential (wet open land) supports Merauke Regency to be the development of one of the national rice production centers. The highest rice production centers in Merauke Regency are Tanah Miring, Kurik and Semangga districts. Kurik District has a population of 14,052 people consisting of indigenous tribes namely Malind, Muyu, Mandobo, Awuyu, Yagai and Asmat. The immigrant community in Merauke Regency is dominated by the Bugis, Javanese, Moluccas and Buton (Badan Pusat Statistik, 2018).

The sustainability of less considered land resources results in high-quality land being reduced and humans increasingly relying on marginal land resources. The causal factor of rice land to non rice land are lower productivity, low quality of land and higher economic values of land (Sumarno, 2006). This has implications for reduced food security, the level and intensity of heavy pollution and other environmental damage.

Indonesia's environmental sustainability in utilization results in community disobedience. Land use that is not in accordance with the potential of land due to lack of knowledge also causes problems. Land potential in Kurik, Merauke supports efforts to increase food sovereignty as one of the political agendas of President Jokowi and Vice President Jusuf Kalla. The author raised the research object related to sustainable Rice Field Productivity (Padi) in Dsitrik Kurik Merauke Regency.

### *1.1. Goals and External Targets*

Based on the background and problems that arise, the purpose of this study is as follows:

1. Knowing the condition of the productivity value of kurik district rice rice as a criteria for sustainable rice field direction
2. Know the distribution of sustainable rice fields based on actual land criteria.

### *1.2. Benefits of Research*

The benefits of the results of the research is a design of rice-specific agricultural land management in Harapan Makmur Village Kurik District Merauke District of Papua, expected to facilitate farmers in the management of agricultural land by using Geographical Information System technology.

## 2. Library Review

### *2.1. Farm Land*

According to Indonesian Law No. 41/2009, agricultural land is a field of land used for agricultural cultivation. Agricultural land is used as a medium for planting certain commodities in order to meet human food needs (UU Republik Indonesia Nomor 41, 2009). Commodity crops replace the natural vegetation of the land thus generating economic value. Agricultural land consists of rice fields and non-rice fields (dry land). Rice fields are farmland that has a flat land surface and is limited by ripens so that it can be planted with food crops (rice) with a system of puddles / rain or intermittent irrigation.

### *2.2. Rice Plants*

Rice goes through several phases of growth until it produces grain to then be ground and produce rice ready for consumption. There are three main phases of rice growth, namely (1) vegetative, (2) reproductive, and (3) maturation. The vegetative phase is the initial phase of growth of vegetative organs until the formation of malai. Reproductive phase is the primordia phase until flowering, in the tropics this phase generally takes 35 days. The last phase is the maturation phase which is the stage from flowering to mature grain. The length of this phase is generally 30 days. The time it takes for rice in each phase varies because it is influenced by physical factors as well as rice varieties.

### *2.3. Geographic Information Systems (GIS)*

Sub systems of GIS from input data, data manipulation and analyst, data management, and output data processed by GIS to manipulate, analyze, visualize, and produce geographic information outputs equipped with their attributes. A digital cadastral map can be the basis for additional thematic layers, successively converting to a complex system for management of admininstrative units (Prahasta, Eddy, 2002).

*2.4. Field Remote Sensing*

Remote sensing is an important tools to upscale yield estimates from farm scales to regional level. Some researcher used remote sensing with rice model for reliable yield estimation. Several countries start to monitoring rice land that needed to synthesize current literature to identify knowledge gaps, to improve estimation accuracies (Sutanto, 2013).

## 3. Research Methods

*3.1. Research Location*

Kurik District was chosen as a research location, because it is the second largest rice producing district in Merauke Regency with the potential of vast rice fields to be developed into agricultural rice fields. Land in the research area is still much that has not been utilized optimally, therefore the location was chosen to realize food self-sufficiency in Indonesia through President Of Indonesia Jokowi's Nawacita program.

*3.2. Research Stages*

There are 3 stages in this research, namely the preparation stage, the implementation stage and the completion stage. Each stage of research has an interrelated process.

3.2.1. Preparatory Stages

Conducting activities to collect information related to research (library studies) as well as data preparation, both main data and supporting data. Research-related information collection activities, namely information related to remote sensing, geographic information systems, sustainable rice fields, criteria for determining sustainable food agricultural land, and other libraries. Information is obtained from a number of books, scientific journals, seminar results, and research-related articles obtained from libraries, internet access and related agencies.

3.2.2. Implementation Stages

The stage of research implementation starts from initial observation and survey, determination of coordinate points, sampling of data in the field, database design, spatial and non-spatial data design, each activity consists of related and sequential processes.

3.2.3. Completion Stage

The completion stage is the end of the research stage where the overall research reporting process is carried out.

## 4. Results of System Design

### *4.1. Proposed System*

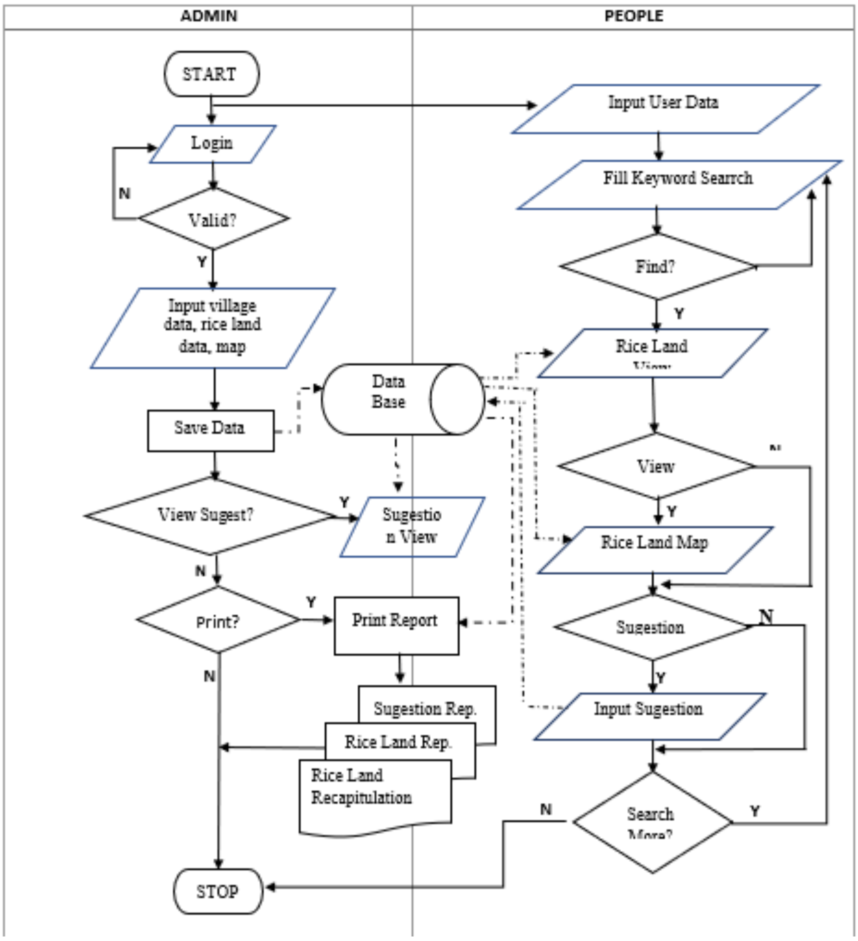


Figure 1 : Proposed System Flowchart

The proposed system has two groups of users, namely Admin and People. Admin is responsible for managing the system. Admins can set user access rights and update data. Admins can also print the required reports. The People can see the information and can provide advice if needed.

### *4.2. Context Diagram*

This Context Diagram illustrates the interrelationship of Admins and Communities using the system.

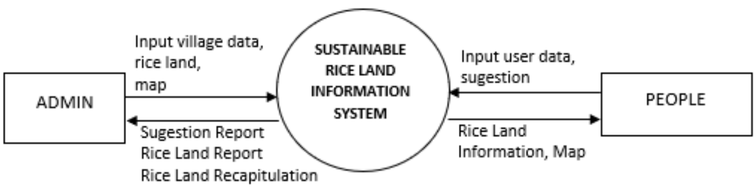


Figure 2 : Context Diagram

### *4.3. DFD Level 0*

DFD Level 0 describes the process details on the system in Context Diagram. This diagram also illustrates the interrelationships between processes and table interrelationships.

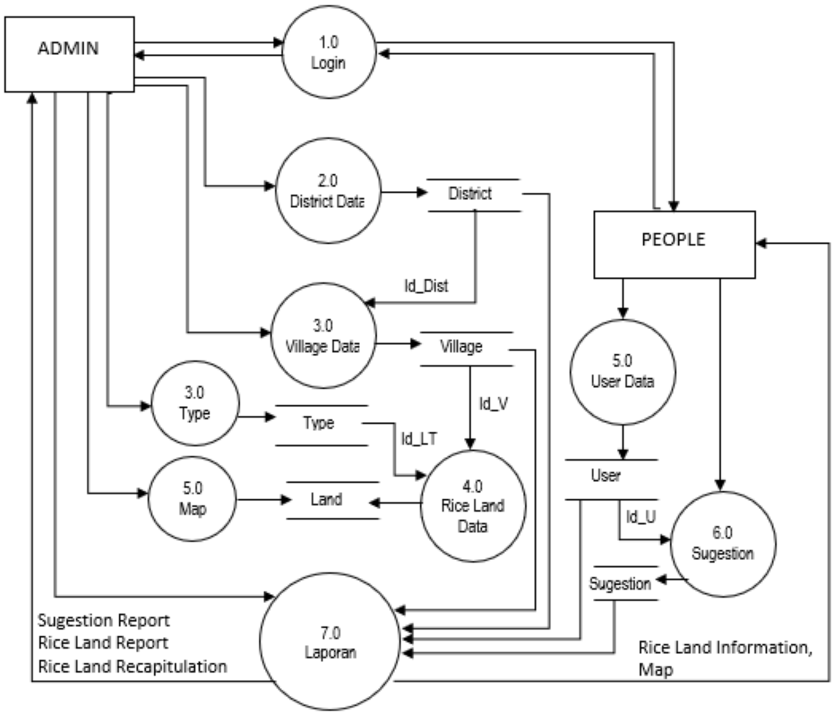


Figure 3 : Context Diagram

*4.4. Entity Relationships*

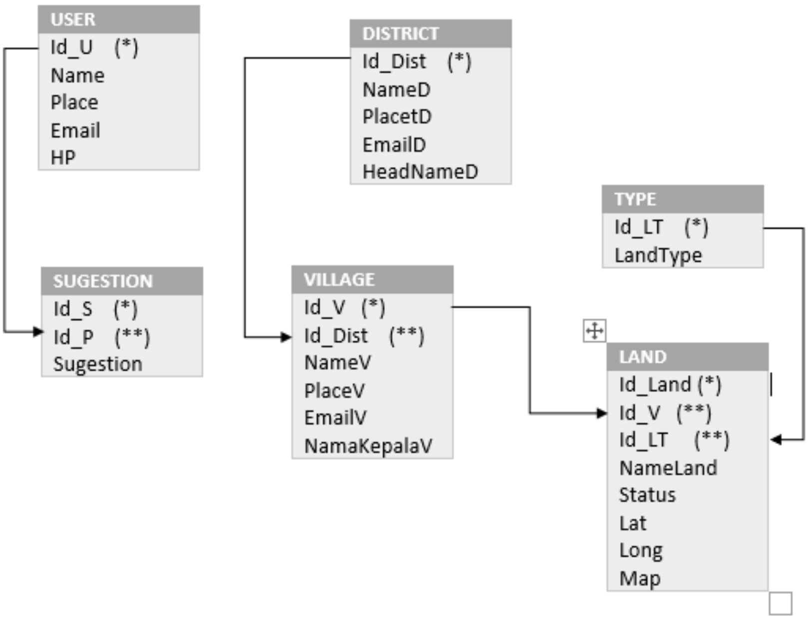


Figure 4 : Entity Relationships

This Entity Relationships describes the interrelationships of tables in the data base. User table is connected only with Sugestion tables. District Table is related to Village table, Villlage Table is related to Land table, and Land table is related to Type table.

*4.5. Interface Form Design*

The interface design on the proposed system is useful for giving an idea of the menu display plan to be used for data input dialogs. The data input dialog design is as follows:

4.5.1. Login Dialog

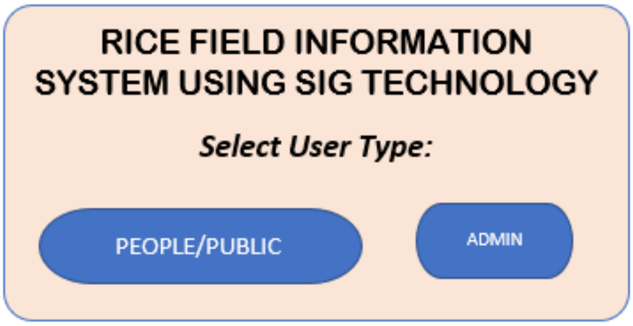


If the user selects Public/General then the user will go to the user data input menu. If the user selects Admin then the user will go to the Admin login menu

4.5.2. Land Information Search Dialog

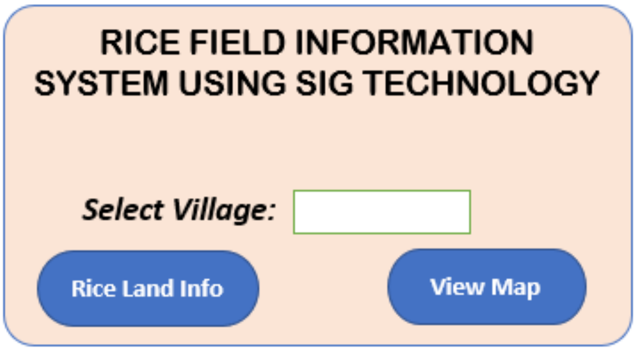


*4.6. Output Design (Output)*

4.6.1. View of Rice Field Information

Kampung Data Input dialog can be opened by General Users / public

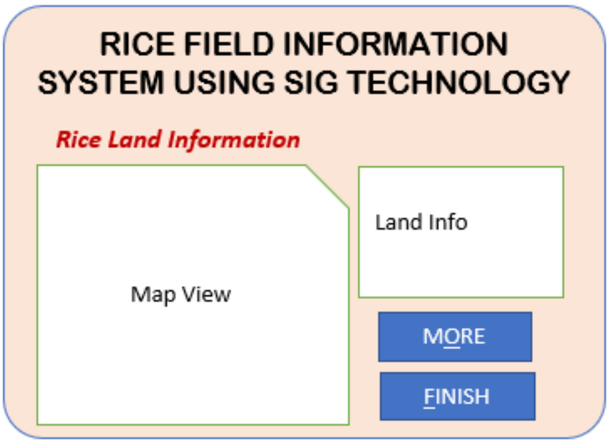


4.6.2. Design of Report

LOGO

**RICE FIELD INFORMATION SYSTEM USING SIG TECHNOLOGY**

***PEOPLE'S SUGESTION REPORT***

Date

| No | Guest Name | Date | Sugestion |
|---|---|---|---|
| 1 | | | |
| 2 | | | |

People Sugestion Reports can only be opened and printed by ADMIN Users.

4.6.3. Rice Field Report Plan

LOGO

**RICE FIELD INFORMATION SYSTEM USING SIG TECHNOLOGY**

***RICE LAND REPORT***

Date: dd/mm/yyy

| No | Land's Name | Village | Land's Type | Width (Ha) | Status |
|---|---|---|---|---|---|
| 1 | | | | | |
| 2 | | | | | |

The Rice Field Report can only be opened and printed by Admin users.

4.6.4. Land Area Recapitulation Plan

LOGO

**RICE FIELD INFORMATION SYSTEM USING SIG TECHNOLOGY**

***RICE LAND RECAPITULATION***

Date: dd/mm/yyyy

| No | Village | Land's Type | Width (Ha) |
|---|---|---|---|
| 1 | | | |
| 2 | | | |
| | | **Total Land** | **99999999** |

Rice Land Recapitulation can only be opened and printed by ADMIN Users

## 5. Conclusions

1. All plans for the management of rice fields in the Harapan Makmur Village of Kurik District have been implemented as can be seen in Chapter V results and discussions.
2. This phase one internal research is devoted to the design of rice field management in Harapan Makmur Village of Kurik District.

## References


Asma Th. Ibraheem (2012). Development of Large-Scale Information System (LIS) by sing GIS and Field Surveying. Department Of Civil Engineering Nahrain University, Baghdad, Iraq

Badan Pusat Statistik (2018). *Merauke In Numbers.* PEMDA Kabupaten Merauke.

Barus B, Panuju, Iman, Triasongko, Gandasasmita, dan Kusumo (2011). *Mapping the Potential for Rice Field Conversion in Relation to Sustainable Agricultural Land with Spatial Analysis*. [Paper Presentation] In *Seminar dan Kongres HITI X*

Claudia Pahl-Wostl (2019). Governance of The Water-Energy-Food Security Nexus: A Multi-level Coordination Challenge. Environmental Science & Policy, Vol 92 p 356-367

Javier Giovanny AH, Lida Paola PG, Javier EV (2017). Growth and Productionof Rice (Oryza Sativa L.) Under Different Fertilization Plans With Silicon. Journal Ingenieria Investigation, Vol 7 No 1 p 7-15

Kementrian Pertanian-Skretariat Jendral (2013). The Statistis Of Rice Field Raw Area and Rice Harvest Area. *http://eksim.pertanian.go.id/publikasi302-statistik-luas-baku-lahan-sawah-dan-luas-panen-padi.html*

Nurliani, Ida Rosada (2016). Rice-field Conversion and It's Impact On Food Availability. Journal Agriculture And Agricultural Science Procedia, Vol 19, Pages 40-46.

Permentan No: 07/Permentan/Ot.140/2/2012 (2012). *Sustainable Food Agricultural Land Specifications*. Menteri Pertanian Republik Indonesia. Jakarta

Prahasta, Eddy (2002). *Geographics Information System Conceps*. Informatika, Bandung.

Sartohadi, J dan Putri, R.F. 2008. *Evaluation of Land Degradation Potential Using Analysis of Land Capability and Population Pressure on Agricultural Land in Kokap District of Kulon Progo Regency*. Journal Of Forum Geografi, Vol. 22, No. 1. Fakultas Geografi Universitas Gadjah Mada. Yogyakarta

Sumarno (2006). *Sustainable Rice Production System with the Implementation of the Sustainable Green Revolution.* Iptek Tanaman Pangan (1)

Sutanto (2013). *The Method Of Remote Sensing Research*. OMBAK, Yogyakarta

T. Subramani, G. Raghu Prakash (2016). Rice Base Irrigated Agriculture Using GIS. IJETTCS, Vol 5 issue 3

UU Republik Indonesia Nomor 41 (2009). *Protection of Sustainable Food Agricultural Land. Pasal 9 Ayat 5.*

The Asian Institute of Research
Engineering and Technology Quarterly Reviews
Vol.5, No.1, 2022: 9-16
ISSN 2622-9374


# Influence of Masonry Infill Panels Mechanical and Physical Properties on the Seismic Performance of RC Frame

Horatiu-Alin Mociran[1]

[1] Faculty of Civil Engineering, Technical University of Cluj-Napoca, Cluj-Napoca, Romania

Correspondence: Horatiu-Alin Mociran, Faculty of Civil Engineering, Technical University of Cluj-Napoca, Cluj-Napoca, St. Memorandumului 28, Romania. E-mail: horatiu.mociran@mecon.utcluj.ro

**Abstract**
The paper investigates numerically the influence of masonry infills properties on the seismic response of RC frame structures. A five-story plane RC frame with infill panels (benchmark), part of a residential building, situated in Piatra Neamț, was considered for this aim. The benchmark was designed according to the current design practice and based on current Romanian seismic design codes, thus the infills were modelled as uniformly distributed gravitational loads on beams. Two more cases of the same structure were examined: case 1, with infill panels made of hollowed ceramic blocks and case 2, with infills made of AAC. In both cases, infills panels were modelled through diagonal struts. Comparative nonlinear time history analyses of the structures were performed. In both cases, compared to benchmark, the results show that peak inter-story drift ratios, peak bending moments of columns and beams were reduced significantly, peak axial forces of columns had a small variations and base shears were slightly increased.

**Keywords:** Infill Panel, RC Frame, Mechanical Property, Diagonal Strut, Time History analysis

## 1. Introduction

In Romania, as well in other earthquake prone countries, infill panels are frequently used in the case of multi-stories buildings with RC frame structures due to their advantages: thermal conductivity, low bulk density and an affordable cost (Dautaj et al., 2018; Mociran & Cobârzan, 2021a; Pallares et al., 2021).

Major seismic events of the past have shown that although RC frame structures have an adequate response, non-structural components of buildings (infill panels, mechanical equipment etc.) have suffered important damages (Dolce & Goreti, 2015). Consequently, material damages have been much more significant in the case of non-structural components, in comparison with those of the structure (Gaudio et al., 2016; Trapani et al., 2020). In addition, the collapse of non-structural components is a danger to people's lives.

Field observations of buildings affected by earthquakes, as well as numerous experimental and numerical studies have highlighted that masonry infills panels in full contact with the surrounding frames, interact with them, significantly influencing the seismic response of the structure (Alwashali, 2019; Fiore et al., 2012). The masonry infills panels provide the structure with extra strength and stiffness, which depend on the mechanical properties of the infill panels and on the ratio between their strength and the strength of the frames (Penelis & Penelis, 2014; Peng et al., 2018; Perrone et al., 2017; Santos, 2007).

The paper aims to investigate numerically the influence of masonry infills properties, for two types of masonry units frequently used in Romania, on the seismic performance of a typical low-rise RC frame structure, located in a moderate seismic area.

**2. Description of Case Studies**

A five-story plane RC frame (benchmark), part of a residential building, has been chosen for this study. The building is in Piatra Neamț, a moderate seismic zone of Romania, and has been designed by Mociran and Cobîrzan (2021b), according to Romanian seismic design code, (*P100-1/2013*, 2013), and Romanian standard for design of concrete structures, *(SR EN 1992-1*, 2006), considering a dissipative behavior with ductility class medium (DCM). It is important to highlight that in the design of benchmark structure, the infills have been modelled as uniformly distributed gravitational loads on beams, according to current design practice. The geometry of the frame is shown in Figure 1.

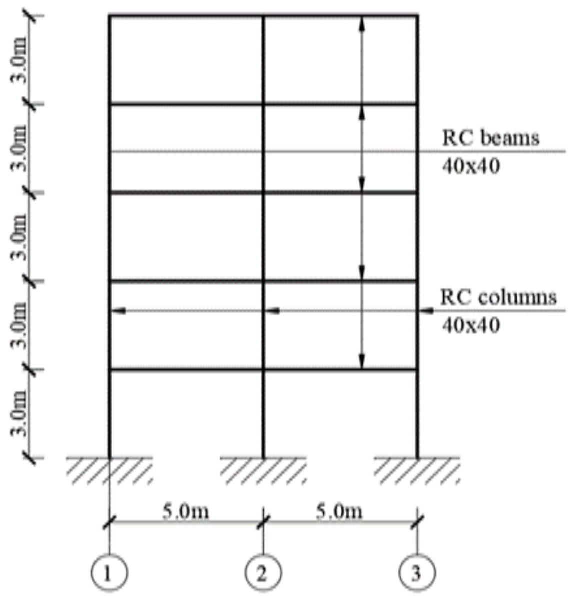


(a)

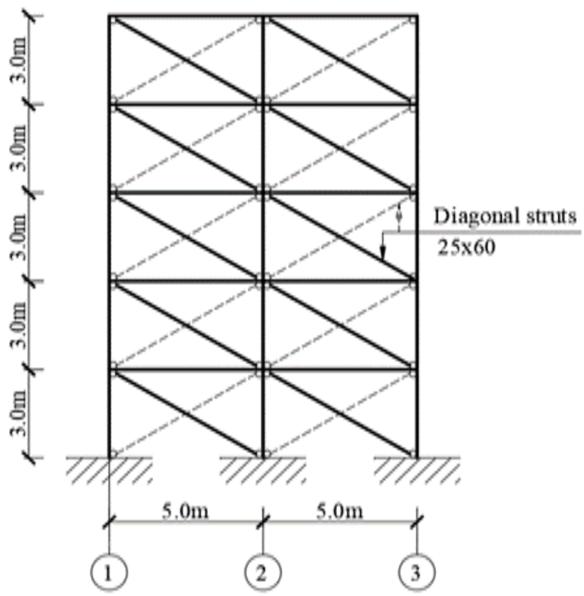


(b)

Figure 1: Elevation view of RC frame: benchmark (a), with infill panels (b)

The seismic load has been established by modal response spectrum analysis. The main parameters of the design response spectrum have been considered: design ground acceleration ($a_g$=0.25g), corner period ($T_c$=0.7s) and behavior factor (q=4.725). The dimensions of all columns and beams sections are 40x40cm and 30x40cm, respectively. The concrete class C25/30 has been used for all structural members.

To assess the influence of masonry infills mechanical and physical properties on the seismic performance of RC frame structures, two more cases have been considered:

- Case 1, with infill panels made of hollowed ceramic blocks (with normalized compressive strength in the direction of the applied action $f_b = 11.38 N/mm^2$ and density $\rho = 760 N/mm^2$) and mortar class M5 in regular bed joints (compressive strength $f_m = 5 N/mm^2$).
- Case 2, with infill panels made of AAC (with normalized compressive strength in the direction of the applied action $f_b = 5 N/mm^2$ and density $\rho = 600 N/mm^2$) and mortar class M5 in regular bed joints (compressive strength $f_m = 5 N/mm^2$).

It is worth mentioning that the selected types of masonry units are frequently used in Romania for infills. In both cases, the geometry and dimensions of the structural members are the same as in the benchmark. The infill panels have been considered in full contact with the surrounding frames and have been modelled through diagonal struts. The width of all diagonal struts has been taken one tenth of the diagonal of infill frame, according to *P100-1/2013*. Thus, the dimensions of all strut sections are 25x60cm.

By using *CR6/2013* and *P100-1/2013*, the mechanical properties of masonry have been obtained:

- Case 1: design compressive strength in the direction being considered $f_d = 2.1 N/mm^2$, design value of the shear strength under no compression $f_{vd0} = 0.11 N/mm^2$, short term secant modulus of elasticity $E_z = 4000 N/mm^2$.
- Case 2: design compressive strength in the direction being considered $f_d = 1.4 N/mm^2$, design value of the shear strength under no compression $f_{vd0} = 0.07 N/mm^2$, short term secant modulus of elasticity $E_z = 2270 N/mm^2$.

**3. Numerical Analyses**

The seismic performance of the building is assessed by nonlinear time history analyses using *SAP 2000 Educational software*. The seismic input is represented by a set of seven semiartificial accelerograms of Vrancea 1977 NS component type, compatible with the elastic response spectrum for Piatra Neamț. The accelerograms have been generated in *Seismo Match program*. The following seismic response parameters have been investigated: peak inter-story drift ratios at two limit states (Serviceability (SLS) and ultimate (ULS)), peak axial forces and bending moments (at edge and interior columns and beams, respectively) and peak base shears.

*3.1 Inter-story Drift Ratios*

Figures 2 and 3 show the distribution of the peak inter-story drift ratios over the height of structure at SLS and ULS, respectively.

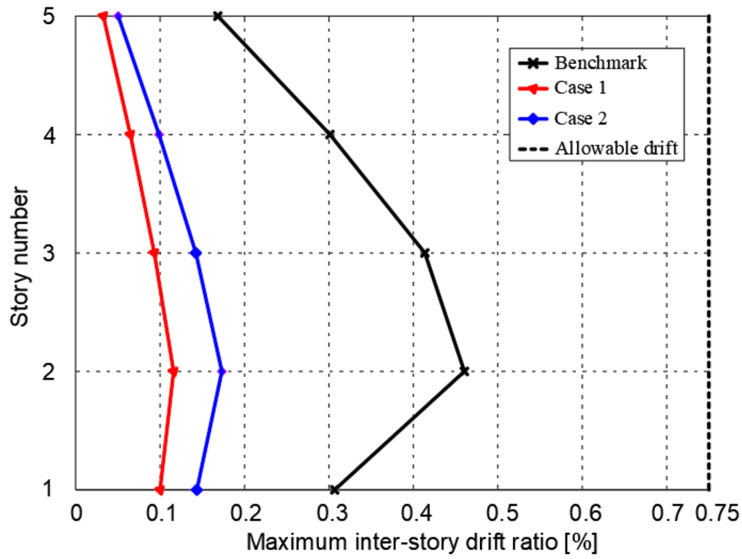


Figure 2: Distribution of peak inter-story drift ratios over the structures' height at SLS

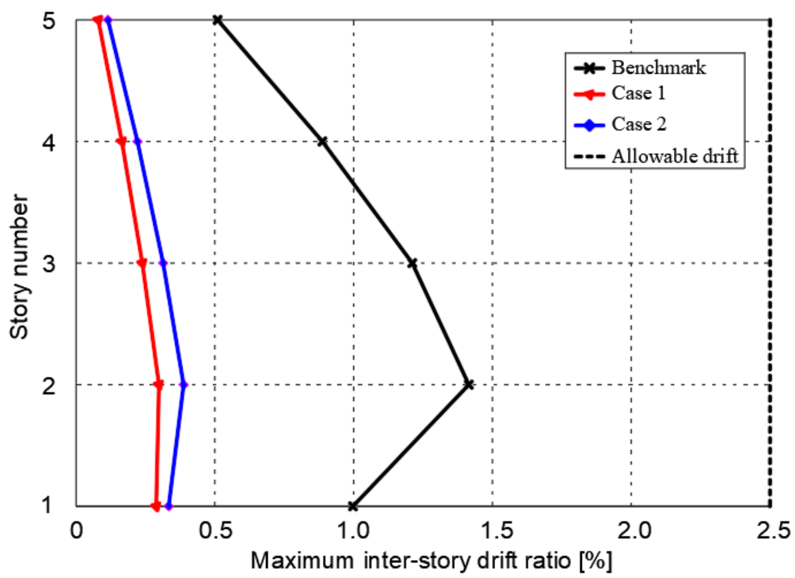


Figure 3: Distribution of peak inter-story drift ratios over the structures' height at ULS

The benchmark structure satisfies the *P100-1/2013* SLS and ULS requirements for inter-story drifts of 0.005h and 0.025h, respectively. In the previous expressions, h represents the height of the story (3m). In the case of benchmark, the maximum magnitude of the inter-story drift ratios has been recorded at the second story, at both limit states. It can be remarked that all inter-story drift ratios of the structures with infills have been significantly reduced compared to benchmark. The reductions slightly increased on the height of the structure from the first to the last story and have been in the range of 65.76-80.59% at SLS and 71-84.3% at ULS for case 1 and 53.15-70.1% at SLS and 66.59-77.5% at ULS for case 2.

*3.2 Axial Forces and Bending Moments*

It is examined the influence of masonry infills mechanical properties on the peak axial forces and moments of an edge and interior column and on the peak bending moments of the beams.

Figures 4 and 5 plot the distribution of maximum bending moments for an edge and interior column, over the height of structures, at ULS.

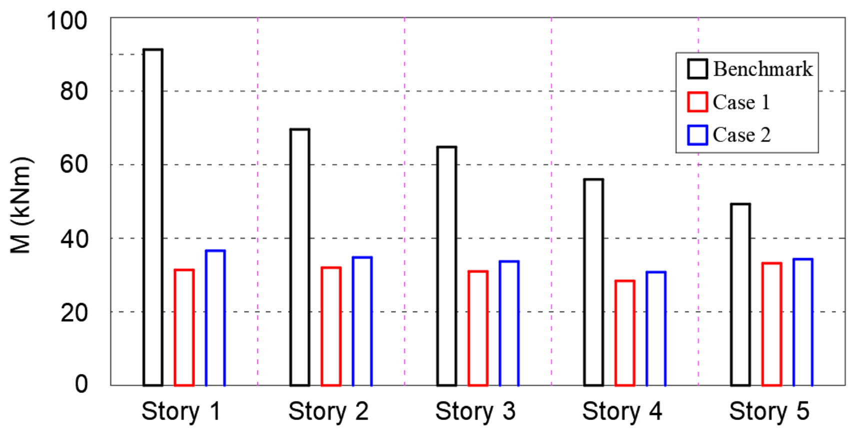


Figure 4: Distribution of peak bending moments for an edge column over the structures' height

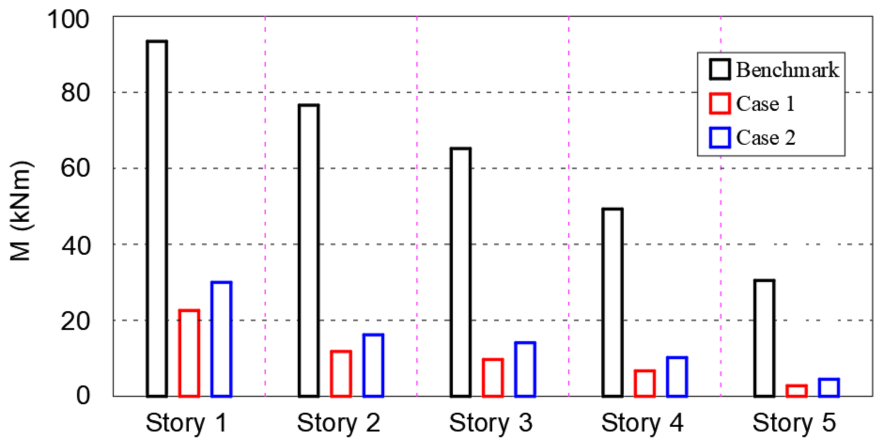

Figure 5: Distribution of peak bending moments for an interior column over the structures' height

In the benchmark, the peak bending moments of the edge columns decrease from the first to the top story. By adding infill panels, the maximum bending moments have been pronouncedly reduced compared to benchmark and became approximately uniformly distributed over the height of the building. Higher reductions (65.66-32.68%) have been achieved for the structure with infills panels made of hollowed ceramic blocks compared to the structure with infill panels made of AAC (59.9-30.4%). In both cases, the maximum reductions took place on the first floor, and the minimum at the top story.

In the benchmark, the peak bending moments of the interior columns decrease from the first to the top story. In cases 1 and 2 important decreases have been obtained, compared to the benchmark: up to 90.86% and up to 85.38%, respectively. Unlike the edge column, the maximum decreases have been recorded at the top story and the minimum decreases at the first story, such that peak bending moments of the cases 1 and 2 decrease from the first to the top story, like in the benchmark.

Figures 6 and 7 show the distribution of maximum axial forces for an edge and interior column, over the height of structures, at ULS.

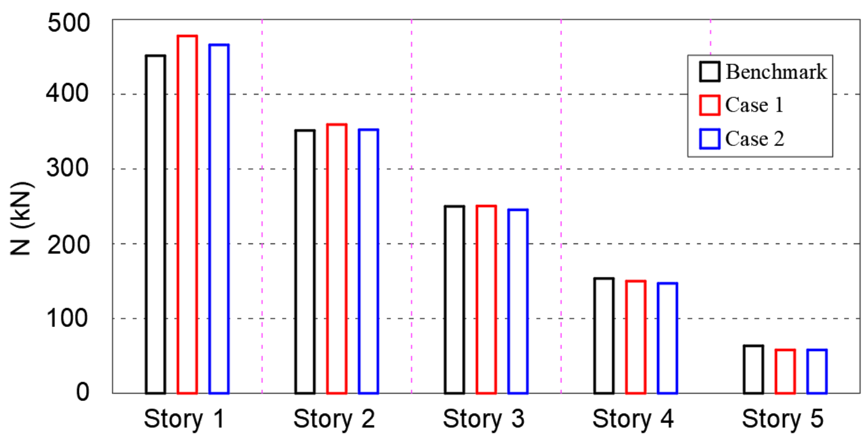

Figure 6: Distribution of peak axial forces for an edge column over the structures' height

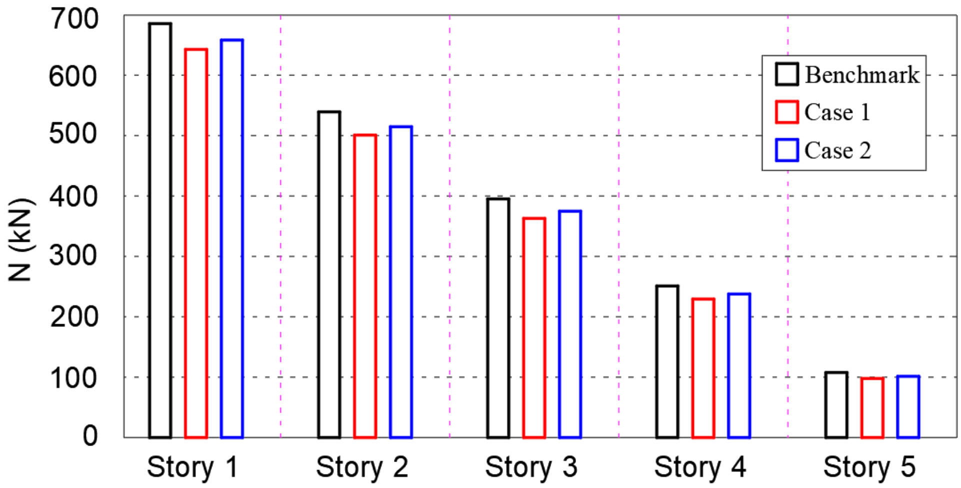

Figure 7: Distribution of peak axial forces for an interior column over the structures' height

In the case of columns, insignificant variations of bending moments have been observed compared to benchmark. For edge column, small increases have been noticed in the lower stories (up to 5.87% in case 1 and up to 2.84% in case 2) and slight decreases in higher stories (up to 8.3% in case 1 and up to 8.52% in case 2). For interior column, slight decreases have been seen (up to 9.27% in case 1 and up to 6.3% in case 2).
Figure 8 illustrates the distribution of the maximum bending moments at beams, over the height of structures, at ULS.

In the benchmark, the peak bending moments of the beams decreases from first story to top story. It can be observed that all bending moments of the structures with infill panels have been reduced compared to benchmark by up to 49.53% in case 1 and by up to 73.78% in case 2. Higher reductions have been achieved at the lower stories, and lower reductions at upper stories.

By analyzing the obtained results, it can be concluded that by explicit modeling of infills panels through diagonal struts, the behavior of structure changes from a moment resisting frame into a truss type structure.

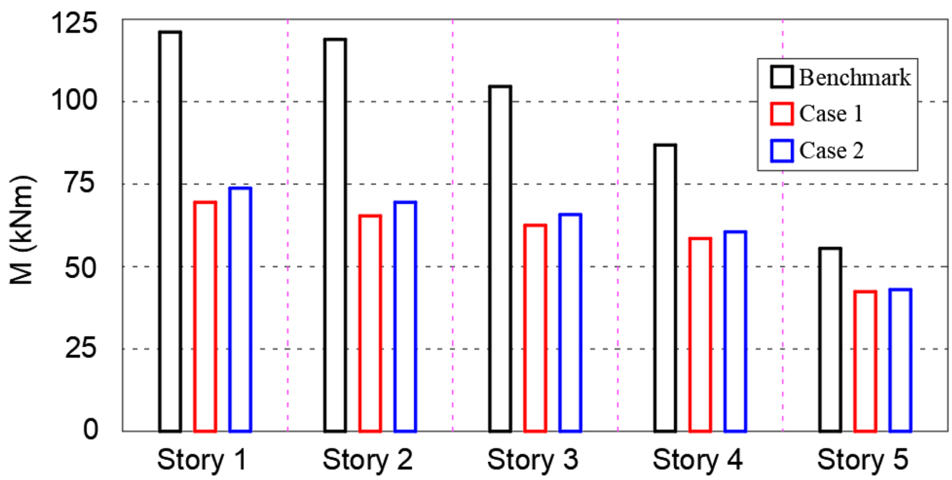

Figure 8: Distribution of peak bending moments for a beam over the structures' height

*3.3 Base Shears*

Figure 9 displays the average value (of the seven time history analyses) of the maximum values of the base shears at ULS, for the considered cases.

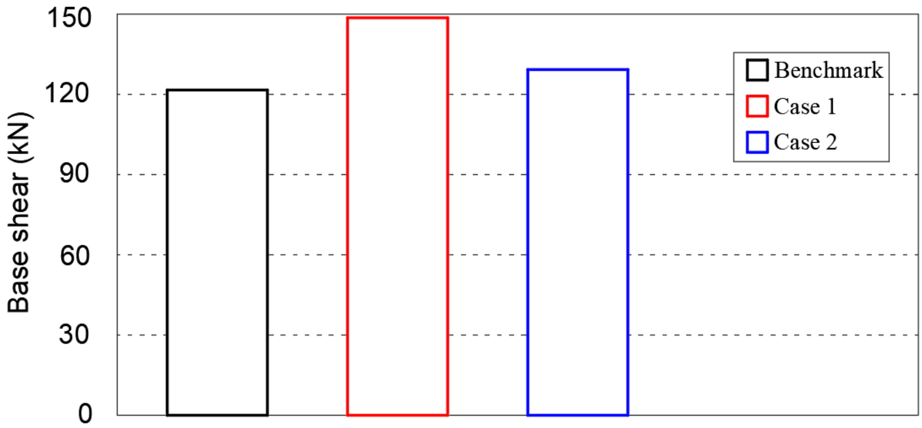


Figure 9: Peak base shears

It can be observed, that by adding infill panels to the benchmark, the values of the maximum base shears have been increased, since the stiffness of the benchmark has been increased. The maximum base shear has been increased by 22.19% in case 1 and by 6.25% in case 2.

**4. Conclusions**

The following conclusions can be drawn from the present numerical study:

- The peak inter-story drift ratios have been substantially reduced at all stories of the structures by 65.76%-80.59% at SLS and by 71%-84.3% at ULS in case 1 and by 53.15%-70.1% at SLS and by 66.59%-77.5% at ULS in case 2, compared to benchmark. This is explained by the supplemental stiffness added by the infill panels.
- The peak bending moments of the edge and interior columns have been reduced at ULS by 32.68%-90.86%, in case 1 and by 30.4%-85.38%, in case 2, compared to benchmark. At the same time, the values of axial forces in the columns had a small variation (up to 10%), compared to benchmark. The sizes of the sections of structural members can be diminish by considering the internal forces and moments obtained by explicit modeling of infill panels through diagonal struts, with benefits on execution costs.
- The magnitude of reductions of maximum inter-story drift ratios and of peak bending moments of columns and beams is highly influenced by values of elastic modulus and bulk density of masonry.
- Peak base shears have been increased by 22.19% in case 1 and by 6.25% in case 2, compared to benchmark. Neglecting this additional base shear at the design of structure can lead to brittle failure of columns at their ends.

The results obtained in this study have pointed out the importance of modeling the infill panels through diagonal struts and have shown that the seismic performance of the building depends on the mechanical and physical properties of the materials used for infills.

**References**

Alwashali, H., Sen, D., Jin, K., & Maeda, M. (2019). Experimental investigation of influences of several parameters on seismic capacity of masonry infilled reinforced concrete frame. *Engineering Structures*, 189, 11-24. https://doi.org/10.1016/j.engstruct.2019.03.020

Dautaj, A.D., Kadiri, Q., & Kabashi, N. (2018). Experimental study on the contribution of masonry infill in the behavior of RC frame under seismic loading. *Engineering Structures*, 165, 27-37. https://doi.org/10.1016/j.engstruct.2018.03.013

Dolce, M., & Goreti, A. (2015). Building damage assessment after the 2009 Abruzzi earthquake. *Bulletin of Earthquake Engineering*, 13, 2241-2264. https://doi.org/10.1007/s10518-015-9723-4

Gaudio, C.D., Ricci, P., Verderame, G.M., & Manfredi, M. (2016). Observed and predicted earthquake damage scenarios: the case study of Pettino (L'Aquila) after the 6th April 2009 event. *Bulletin of Earthquake Engineering*, 14, 2463-2678. https://doi.org/10.1007/s10518-016-9919-2

Fiore, A., Netti, A., & Monaco, P. (2012). The influence of masonry infill on the seismic behaviour of RC frame buildings. *Engineering Structures*, 44, 133-145. https://doi.org/10.1016/j.engstruct.2012.05.023

Mociran, H.A., & Cobîrzan, N. (2021a). Assessment of seismic performance of RC frame structure with masonry infill panels partially uncoupled from the surrounding frame members. *IOP Conference Series: Materials Science and Engineering*, 1138 (012029), doi:10.1088/1757-899X/1138/1/012029

Mociran, H.A., & Cobîrzan, N. (2021b). Pushover analysis of R.C. framed structures with infill panels made of masonry having various properties. *IOP Conference Series: Materials Science and Engineering*, 1138 (012030) doi:10.1088/1757-899X/1138/1/012030

Pallares, F.J., Davia, A., Hassan, W.M., & Pallares, L. (2021). Experimental and analytical assessment of the influence of masonry façade infills on seismic behavior of RC frame buildings. *Engineering Structures*, 235, 112031. https://doi.org/10.1016/j.engstruct.2021.112031

Penelis, G.G, & Penelis, G.G. (2014). *Concrete buildings in seismic regions*. CRC Press.

Peng, Q., Zhou, X., & Yang, C. (2018). Influence of connection and constructional details on masonry infilled RC frames under cyclic loading. *Soil Dynamics and Earthquake Engineering*, 108, 96-110. https://doi.org/10.1016/j.soildyn.2018.02.009

Perrone, D., Leone, M., & Aielo, M.A. (2017). Non-linear behaviour of masonry infilled RC frames: Influence of masonry mechanical properties. *Engineering Structures*, 150, 875-891.

Romanian Ministry of Regional Development and Public Administration. (2013). *Seismic design code. Part I: Design rules for buildings* (P100-1/2013).

Romanian Standards Association. (2006). *Eurocode 2: Design of concrete structures – Part 1-1: General rules and rules for buildings* (SR EN 1992-1-1).

Santos, S.P. (Eds.). (2007). *Enclosure masonry wall systems worldwide*. CRC Press.

SAP 2000 educational version.

SeismoMatch educational version.

Trapani, F.D., Bolis, V., Basone, F., & Preti, M. (2020). Seismic reliability and loss assessment of RC frame structures with traditional and innovative masonry infills. *Engineering Structures*, 208, 110306. https://doi.org/10.1016/j.engstruct.2020.110306

Asian Institute of Research
Connecting Scholars Worldwide

The Asian Institute of Research
Engineering and Technology Quarterly Reviews
Vol.5, No.1, 2022: 17-24
ISSN 2622-9374


# Comparison of H.264 and H.265

Milan Jayaratne[1], Pulasthi Dhananjaya Gunawardhana[2], Uthpala Samarathunga[3]

[1,2,3] Department of Information & Communication Technology, University of Sri Jayewardenapura, Pitipana, Sri Lanka

**Abstract**
From the Stone Age to the present day, visual communication can be described as a form of communication that has evolved over various topics, from design to technology. As a result of globalization and the transformation of digital citizenship, services such as the Internet have come into the world. With the advent of mobile phones, computers, and television, more and more people are viewing and sharing videos, the need for a lower cost and higher quality methodology. The H.264 standard was successfully introduced in 2003 as another answer to that problem. The H.264 standard, which supported 1920 x 1080 Full HD resolutions, was no longer more practical than 4K resolutions. A decade later, with the introduction of the H265 in 2013, video usage became even more efficient. This was introduced with the combination of MPEG and ITU-T. H.265 codex mostly targets higher resolution video, such as 4k and 8k. Thru this paper, we are looking into the comparison of the technology used in H.264 and H.265. Specially H.264 and H.265 workflow, Transformation and Quantization techniques used, coding Units, Entropy Coding methods, etc. The quality of the output video is expected to be well preserved to the point where the frame concealment algorithm proposed leaves a very little negative impact on the video

**Keywords:** H.264, H.265, Entropy Coding, Transformation & Quantization

## 1. Evolution of Digital Video Industry in Brief

Man has evolved from Cave paintings from the Stone Age to the present day using various tools and techniques for his visual speech. The world's first motion picture technology, the kineograph, was created by placing a series of photographs on a cylindrical surface. With the invention of the film camera and film, cinema emerged. There were Super 8, 16mm, 35mm, and 65mm films, the most popular 35 film format.

After introducing television to the world in 1928, the world needed a more economical and convenient way of filming than the aforementioned negative films. As a solution to this, the camera and broadcast equipment manufacturers used their technologies to make DV, Mini DV, U-Matic, Beta Cam, and VHS to Create formats using different types of videotapes. Since then, video media has become more and more circulating in society with the help of digitization, which started with the release of the computer, which universities and high-tech research institutes owned, to the general market. Video technology, which had previously been used by the most luxurious elite, began to flow into the middle class.

After digitization, the media that use video in the general society can be divided into two main categories. Namely, online media and offline media. Examples include VCDs, DVDs, digital displays, video players, offline media and social media, e-learning, video conferencing, and smartphone online media. Playing (Offline Applications) or streaming (Online Applications) video with more excellent quality and the lower cost was a challenge in these wide-ranging digital video applications, and H264 and MPEG-4 compression methods were the perfect solutions.

## 2. History of the H.26x series

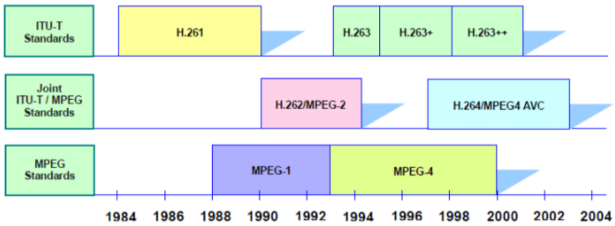


Figure 1: H.6x Family

The first compression seen in the H26x generation is the H261 compression scheme. H.261 is the International Telecommunication Union (ITU) T video coding standard approved in November 1988 (Hanzo, 2007). It was the first video codec that was useful.

H.261 was initially developed for transmission over ISDN lines, and the data rate is a multiple of 64 kbps. The encoding algorithm is designed to work with video bitrates from 40kbps to 2Mbps. H.261 supports two video frame sizes: CIF (352x288 luminance with 176x144 chroma) and QCIF (176x144 with 88x72 chroma) with 4:2:0 sampling. There is also a backwards-compatible trick to transfer still images at 704x576 luminance resolution and 352x288 chrominance resolution (Mahammad, 2017). H.263 is a video compression standard developed initially as a low bitrate compression format for video conferencing. It was developed by the ITU Video Coding Experts Group (VCEG) as part of a project that ended in 1995/1996 as part of the H.26x video coding standards suite in the ITUT domain.

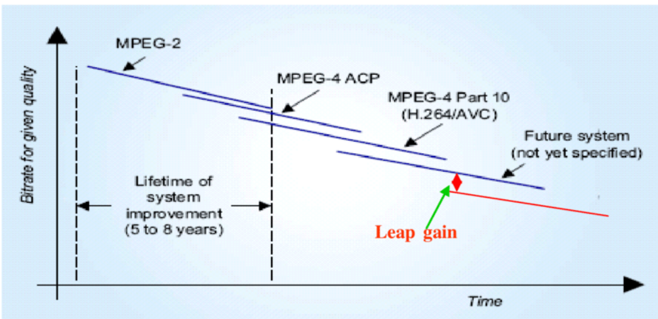


Figure 2: H.26x Family Improvement

## 3. Basics of H264

The H264 is arguably the most widely used video compression in the world. The H264 compression is used in broadcast, streaming, and even everyday optical discs. The H264 standard was developed by the ITU-T Video Coding Expert Group (VCEG) of the 16th Study Group with ISO / IEC JTC1 Moving Picture Experts Group (MPEG) (Recommendation ITU-T H.264, 2016). H264 Compression consists of 3 main techniques: Prediction, Transformation and Quantization, and entropy coding which is called Block-Based hybrid video coding.

*3.1. Block-Based hybrid video coding*

A digital video signal consists of an image sequence called a frame. This frame consists of pixels spread across two dimensions and is available in 3 main light colours: red, green, and blue. Normally this RGB pixel data is converted to Y, U, V. In this Block - Base coding system, the pixels in a complete frame are fragmented into macroblocks. There will be 16x16 size pixels as Y components and 8x8U and V components (Bull, 2014).

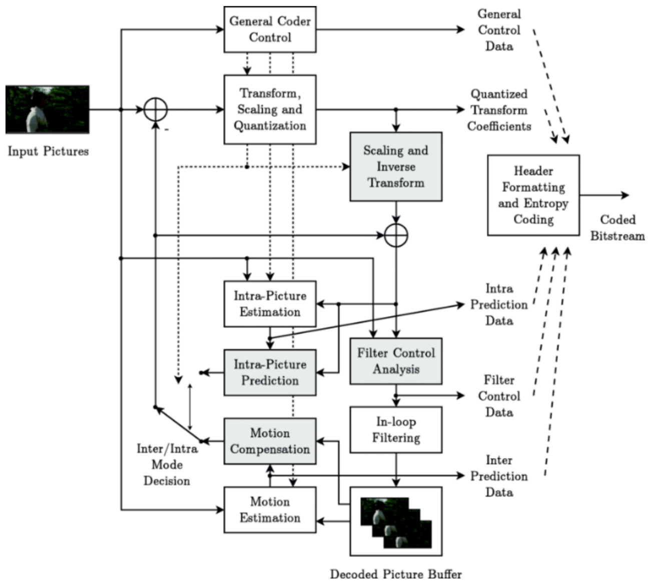


Figure 3: H.264 workflow

## 4. Basic Video Coding Techniques

*4.1. Prediction*

Prediction tries to find a reference Macroblock that is similar to the current Macroblock under processing so that, instead of the whole current Macroblock, only their (hopefully small) difference needs to be coded. Depending on where the reference Macroblock comes from, prediction is classified into inter-frame prediction and intra-frame prediction. In an inter-predict (P or B) mode, the reference Macroblock is somewhere in a frame before or after the current frame, where the current Macroblock resides. It could also be some weighted function of Macroblocks from multiple frames. In an intra-predict (I) mode, the reference Macroblock is usually calculated with mathematical functions of neighbouring pixels of the current Macroblock (Xu, 2010).

.

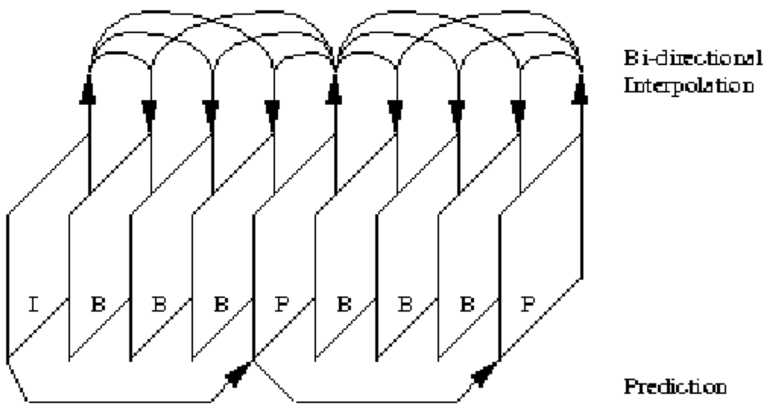


Figure 4: I, P, B frames

*4.2. Compensation*

According to the prediction, there are two kinds of compensation, Intra Compensation & Inter Compensation. Intra Compensation regenerates the current macroblock pixels on of 13 modes. 9 Intra 4x4 for chrominance & 4 Intra 16x16 for Luminance.

Inter Compensation (Motion Compensation) is used in a decoding path to generate the inter-frame motion predicted (estimated) pixels by using motion vectors, reference index and reference pixel from inter prediction. inter compensation also allows variable block size, multiple reference frames and quarter-pixel accurate motion vector (Wang, 2005)

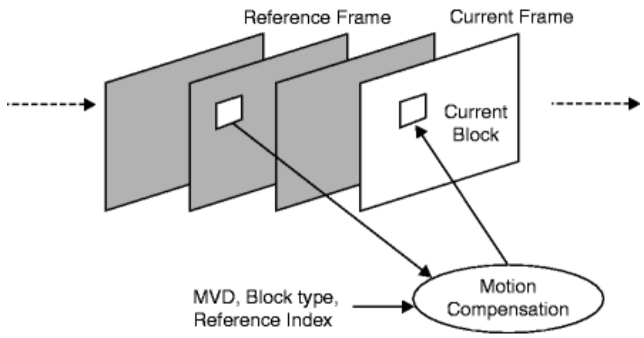


Figure 5: H.264 Motion Compansation

*4.3. Transformation & Quantization*

The difference between the actual and predicted data is called residual error data. Discrete Cosine Transform (DCT) is a popular block transform for image and video compression. Transforms residual data from a time-domain representation to a frequency domain representation. Because most images and videos are low-frequency data, DCT can centralize encoding information.

The main function of quantization is to reduce the transformed coefficients and the encoding information. Because the human eye is less sensitive to high-frequency image components, some video and image compression standards may use higher scaling values (quantization parameters) for high-frequency data. The h.264 standard uses the 4x4 integer DCT (Chen, 2006)

*4.4. Entropy Coding*

The entropy encoder is responsible for converting the syntax elements (quantized coefficients and other information like motion vectors, prediction modes, etc.) into a bitstream, and then the entropy decoder can retrieve the bitstream syntax of the elements. H.264 introduces two entropy coding methods. Context Adaptive Variable Length Coding (CAVLC) and Context Adaptive Binary Arithmetic Coding (CABAC) (Mian, 2007)

**5. Basics of H265**

The advent and adoption of 4K technology was a critical factor in the development of H.265. In a nutshell, 4K cameras can produce files 4x larger than regular 1080p (Full HD) files, which makes a huge difference in handling this data.

Until now, it was compressing 4K camera footage to a lower bitrate for faster streaming, and lower storage requirements often result in lower image quality than lower-compression HD footage. H.265 would theoretically eliminate this problem. However, the "theoretically" section is important because of the drawbacks associated with the H.265 implementation. H.265 or high-performance video encoding (HEVC) is sometimes the latest standard in the form of video coding and is also a promotion of H.264, which is also an extended video encoding (AVC).

The final goal of this standard is to provide the same or improved image quality. However, compressive efficiency should be improved easier to manage large data files and reduce total storage loads.

The quote varies depending on the potential savings, but several factors can affect the actual results; H.265 can reduce the bit requirements, and the relevant warehouse requirements are about 30%, and related warehouse requirements are about 30%, And related warehouses requirements are video quality. Likewise, when saving the same bit rate, close image quality is provided.

The difference is that H.265 is more aggressive in this process. In addition to changing the size from 16 x 16 pixels up to 64 x 64 or extending the checked area for pattern matching, features such as motion compensation, spatial prediction, and adaptive sampling offset (SAO) image filtering are included in compression algorithms.

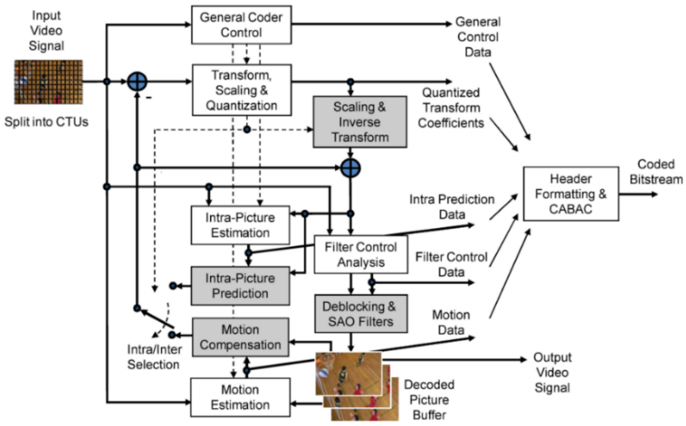


Figure 4: H.265 workflow

The H.265 system is more advanced in every aspect than the H.264 compressor system. Introducing a new hierarchical syntax representation and an Adaptive Loop Filter.

**6. The Coding Tree Block**

The base of the coding layer in H.264 is the macroblock, which contains a block of 16×16 luminance samples and, in the usual case, 4:2:0 chroma sampling, two 8×8 d-blocks of colour, respectively (Gary and Sullivan 2012). Response; while the same structure in HEVC is a coding tree unit (CTU), whose size is chosen by the encoder and can be larger than a traditional macroblock. The CTU consists of a luma CTB and the corresponding colour CTBs and syntax elements. The L×L size of the luma CTB can be chosen as L=16, 32, or 64 samples, with larger sizes generally allowing for better compression. HEVC then supports partitioning the CTB into smaller blocks using a quadtree-like signal and tree structure.

*6.1. Coding Units (CUs) and Coding Units (CBs):*

The quadtree syntax of a CTU defines the size and position of the luma and chrominance CBs. The root of the quadtree is associated with the CTU. Therefore, the size of the luminance CTB is the largest size supported for the luminance CB. The division of CTU into CB of luma and chrominance is signalled together. One luma CB and usually two chrominance CBs together with the appropriate syntax form a coding unit (CU). A CTB can contain only one CU or can be partitioned to form multiple CUs, each CU having an associated partition with a tree of prediction units (PUs) and transformation units (TUs).

*6.2. Intra Prediction*

Intra prediction algorithms are used to predict pixel values based on reference samples of available neighbouring blocks in the current frame. Intra Predictions contains 4 basic modes (Abramowski, 2011). There are;

**Horizontal -** The pixel prediction is equal to the rightmost sample in the same row in the left neighbour block.
**Vertical -** The pixel prediction is equal to the bottom sample in the same column in the upper neighbour block.
**DC -** The pixel prediction is equal to the normalized sum of the horizontal and vertical prediction.

Angular (31 Directions) - The most difficult mode requires three steps. First, the horizontal component is defined as the sample of the upper neighbour selected by the prediction angle. The scaling factor is computed based on the current row of pixels in the prediction unit. Pixel prediction equals the normalized sum of each horizontal component multiplied by each scaling factor.

*6.3. Inter Prediction*

The high-efficiency standard of video encoding (HEVC) improves the previous compression efficiency using a new tool and a more flexible coding structure such as Tree-Based coding block (CB / CTB – Coding Tree Blocks), prediction block (PB) and conversion block (TB). To achieve the best Rate-Distortion (RD), the HEVC reference (HM) software uses a thorough process that tests all combinations of the coding structure and test all possible combinations at the lowest RD cost. Although it provides optimal coding efficiency, this process is a significant officer that is responsible for increased calculation complexity from 9% to 502% compared to HEVC encoder, H.264 / AVC used composition.

In inter-frame prediction, the encoder initially checks the Merge / Skip (MSM) mode of CB conceptually similar to H.264 / AVC Pass mode. With MSM, you can receive information about the movement of spatially or temporary adjacent PBS and form a combined area and form joint information about the same mobile information. SKIP mode is considered a particular case of MSM. After testing MSM, the different partition modes are checked in the order shown in Figure, except for CB 8x8, which allows only the first four partition modes (MSM, 2Nx2N, 2NxN and Nx2N) (Correa, 2014).

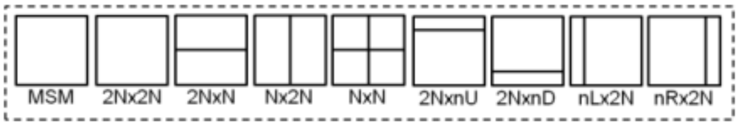


Figure 7: H265 Inter Prediction Modes

*6.4. Transformation & Quantization*

HEVC uses prediction error residual transform coding similar to H.264/AVC. The residual block is split into multiple square transform blocks. Supported transform block sizes: 4x4, 8x8, 16x16, and 32x32. The transformation has two main types. There are Core Transform & Alternative 4 x 4 transform. Two-dimensional transformations are calculated by applying horizontal and vertical 1D transformations direction. The elements of the underlying transformation matrix are inferred by approximating the scaled DCT basis functions, taking into account considerations such as limiting the dynamic range required for the transformation computation and optimizing maximising precision and closeness to orthogonality when matrix entries are specified as integer values.

For quantization, HEVC uses the same Quantization Parameter (QP) control scheme as in H.264/MPEG4 AVC. The QP value range is set from 0 to 51, and incrementing 6 doubles the quantization step size to map the QP values to a logarithmic approximation step size. Quantization ratio matrices are also supported. To reduce the memory required to store frequency-specific values, only quantization matrices of sizes four × 4 and 8 × 8 are used. For transformations larger than 16 × 16 and 32 × 32, an 8 × 8 scaling matrix is sent and applied by splitting the values into groups of 2 × 2 and 4 × 4 coefficients in the frequency subspace - except for those at Position DC position (zero frequency), to which discrete values are sent and applied (Sze, 2014).

### *6.5. Entropy Coding*

Context-adaptive binary arithmetic coding (CABAC) (Sze, 2012) is the technique of entropy coding used in h.264/AVC and also in HEVC. CABAC uses three main functions: binarization, context modelling, and arithmetic coding (Sze, 2014). Binarization: HEVC uses several different binarization processes, including unary (U), truncated unary (TU), kth order ExpGolomb (EGk), and fixed length (FL). This form of binarization was also used in H.264/AVC.

Context Modeling: Context modelling provides accurate probability estimates needed to achieve high coding efficiency. Therefore, it is highly adaptable and can use different context models for different bins, and the probabilities of these context models are updated based on the values of previously encoded bins. Baskets with similar distributions often use the same context model. The context model for each bin can be chosen based on the type of syntax element, the position of the bin in the syntax element (bind X), luminance/chrominance, and neighbour information.

Arithmetic Coding: Arithmetic coding is based on recursive interval division. The range with an initial value of 0 to 1 is divided into two sub-intervals according to the probability of the bin. The encoded bits provide an offset that, when converted to a binary fraction, selects one of two subintervals representing the value of the decoded bin. After each decoded bin, the range is updated to match the selected subplot, and the interval partitioning process repeats. Ranges and offsets have limited bit precision, so whenever the range falls below a certain value, they need to be renormalized to prevent underflow. After decoding each bin, renormalization can occur.

## 7. Conclusion

Table 1: Summary of Comparison About H.264 & H.265

| Technique | H.264 | H.265 |
|---|---|---|
| **Prediction** | Using 16x16 pixles Microblocks. Each consist of 16 x 16 Y ( Luma Components) & 8 x 8 U,V ( Chroma Components) | Using Coding Tree Unit(CTU) Instead of Microblocks and its size L X L Luma can be choosen as a L = 16,32,64 |
| **Transform & Quantization** | Use 4 x 4 Integer DCT | transform matrices were derived by approximating scaled DCT basis functions |
| **Entropy Coding** | CAVLC, CABAC | CABAC |

## References

A. Abramowski, "Towards H.265 video coding standard," Photonics Applications in Astronomy, Communications, Industry, and High-Energy Physics Experiments 2011, DOI: 10.1117/12.905583.

"Advanced video coding for generic audiovisual services", Recommendation ITU-T H.264 [Online].2016. Available: https://www.itu.int/ITU-T/recommendations/rec.aspx?rec=13189.

C.-Y. K. Y.-L. L. Jian-Wen Chen, "Introduction to H.264 advanced video coding," Proceedings of the 2006 conference on Asia South Pacific design automation - ASP-DAC '06, 2006. ISBN: 0-7803-9451-8-/06. https://bunker2.zlibcdn.com/dtoken/901c8067304b524b0c0d610c0a3469fa

D. M. Vivienne Sze, "Entropy Coding in HEVC," Integrated Circuits and Systems, pp. 209-274, 2014. DOI: 10.1007/978-3-319-06895-4_8. https://studylib.net/doc/12703372/entropy-coding-in-hevc-please-share

D. R. Bull, "The Block-Based Hybrid Video Codec," Communicating Pictures, pp. 291-316. 2014. ISBN: 9780124059061

J. J. Y. L. Cai Mian, "An H.264 Video Encryption Algorithm Based On Entropy Coding," Third International Conference on Intelligent Information Hiding and Multimedia Signal Processing (IIH-MSP 2007), 2007. DOI: 10.1109/IIH-MSP.2007.86. https://www.computer.org/csdl/proceedings-article/iih-msp/2007/29940041/12OmNBhZ4kj

J.-R. O. W.-J. H. T. W. Gary J. Sullivan, "Overview of the High-Efficiency Video Coding (HEVC) Standard," IEEE Transactions on Circuits and Systems for Video Technology, vol. 22, no. 12, pp. 1649-1668, 2012. ISSN: 1051-8215. DOI: 10.1109/TCSVT.2012.2221191

M. B. G. J. S. Vivienne Sze, High-Efficiency Video Coding (HEVC) - Algorithms and Architectures, London: Springer International Publishing Switzerland, 2014. ISBN: 978-3319068947.

M. B. Vivienne Sze, "High Throughput CABAC Entropy Coding in HEVC," IEEE Transactions on Circuits and Systems for Video Technology, vol. 22, no. 12, pp. 1778-1791, 2012. DOI:10.1109/TCSVT.2012.2221526. http://www.mit.edu/~sze/papers/sze_tcsvt_2012.pdf

P. A. L. A. L. A. d. S. C. Guilherme Correa, "Four-step algorithm for early termination in HEVC inter-frame prediction based on decision trees," 2014 IEEE Visual Communications and Image Processing Conference, 2014. DOI: 10.1109/VCIP.2014.7051505. https://ieeexplore.ieee.org/document/7051505

P. C. a. J. S. L. Hanzo, Video Compression and Communications, Wiley, 2007. ISBN: 978-0-470-51849-6.

R. W. J. W. Dawen Xu, "Prediction mode modulated data-hiding algorithm for H.264/AVC," Journal of Real-Time Image Processing, no. 4, pp. 205-214, 7. 2010. ISSN: 1861-8200. DOI: 10.1007/s11554-010-0175-4

T.-A. L. T.-M. L. a. C.-Y. L. Sheng-Zen Wang, "A New Motion Compensation Design for H.264/AVC Decoder," 2005 IEEE International Symposium on Circuits and Systems. ISBN: 0-7803-8834-8. DOI: 10.1109/ISCAS.2005.1465646. https://ieeexplore.ieee.org/document/1465646

V. M. V. Farooq Sunar Mahammad, "A Study On H.26x Family Of Video Streaming Compression Techniques," International Journal of Pure and Applied Mathematics, vol. Volume 117 No.10, no. Special, p. 63, 2017. ISSN: 4-3395.DOI: 10.12732/ijpam.v117i10.12. https://acadpubl.eu/jsi/2017-117-8-10/articles/10/12.pdf

The Asian Institute of Research
Engineering and Technology Quarterly Reviews
Vol.5, No.1, 2022: 25-31
ISSN 2622-9374


# An Evaluating of the Broader Economic Benefit of the Medan-Binjai Toll road on National Highway Performance

Ridwan Anas[1], Irwan S. Sembiring[2], Ika Puji Hastuty[3]

[1,2,3] Universitas Sumatera Utara

Correspondence: Ridwan Anas. Email: ridwan.anas@usu.ac.id

**Abstract**
The development of toll roads provides a number of improved services to the road users, connectivity, and their existence can promote the equitable development of a region. The use of toll roads has a variety of impacts on economic issues. The quality of pavement gradually declines along with the increase in pavement service ages and heavy traffic load. After toll operated, over the years the number and characteristics of traffic on national highway have changed. The impact of diverting traffic from the national highway route, will reduce the traffic congestion and improve pavement performance. This paper presents a case study of the wider impact of the toll road investment based on national highway pavement performance and remaining service of life. A scenario is provided to distinguish the traffic diversion from national highway. The imposing toll road would increase the remaining service life of the national highway performance for approximately 6 years from the initial design. Medan-Binjai toll road investment provided high-quality of transport system and on other hand gained a wider benefit for saving the national highway preservation's budget.

**Keywords:** Economic Benefit, Traffic Diversion, Road Performance, Remaining Service of Life

## 1. Introduction

Accessibility and mobility are the objective of almost all the transport investments and will contribute significantly to the economic sector (Mohmand 2016). Indonesia's freight transportation mostly covers up of inland transportation which contributes more than 70% of the total freight movement (Lubis 2005; World Bank 2013). The development of toll roads, intended to boost transport across the nation, to improve connectivity, and their existence can promote the equitable development of a country. New toll road links will increase the road capacity, reduce the travel times and facilitate inland freight transportation, as the traffic volume continues to increase.

The quality of pavement will gradually decline along with the increase in pavement service ages and the heavy traffic load, and it is quite essential to investigate the causes that deteriorate the quality of pavement to select the proper maintenance technique (Hamdi et al. 2015; Yang 2016). Pavement failures in most developing countries have been traced to or combination of traffic load, construction, and climate (Syafriana 2015). Construction of new toll road can have a positive direct impact by reducing the vehicle operating cost and will significantly reduce vehicle traffic and congestion problems on national highways.

After toll operated, over the years the number and characteristics of traffic as a national highway have changed. However, the impact of diverting traffic from the national road route, will reduce the traffic congestion and improve pavement performance (Lozano 2014). Studies in pavement engineering have shown that traffic load is a major factor in design of pavement and has become an important factor causing damage to pavement structure (Yang 2016; Singh 2019).

This paper presents a case study of the wider impact of the toll road investment on a region based on national highway pavement performance and remaining service of life. The information on traffic load required for the pavement design equation. The damaging effect of the traffic loads can be defined by a number of 18-kip equivalent single axle loads (ESALs). The estimation of the remaining service life of the national highway based on AASHTO 1993, by using two scenarios. The first scenario presented the traffic without toll road, and the second scenario presented with toll road operated.

## 2. Literature Review

### *2.1. Road Performance*

The performance of road pavement can be interpreted as the ability of road structural to carry out traffic load and climatic effects over a period of time. Lack of performance service ages becomes the concern primarily because it indicates how far the pavement serviceability could function before rehabilitation work is required to return its function.

Keeping the road pavement in an acceptable level of service is one of the most important aspects, and it can be achieved by having better routine pavement maintenance. A number of factors cause damages to the road pavement such as traffic load, material properties, the environment, and construction practices (Kaare 2012; Jihanny 2018). It is generally used AASHTO to determine a pavement performance as a function of the Pavement Serviceability Index (PSI) and 80 kN ESAL. PSI is stated as a function of pavement condition index and the loss of serviceability (ΔPSI) is the difference between the initial serviceability and the terminal serviceability of the pavement. PSI is expressed as a function of pavement condition index (PCI) and structure condition index (SCI) as shown in equation (Hatmoko 2019).

$$\text{PSI} = f\,(PCI, SCI) < PSIT \quad (1)$$

Where:
PSIT = terminal present serviceability index for design
ΔPSI becomes the main concern, rather than PSI, because it explains how long the pavement could serve the traffic loads and environmental effects before a maintenance is required to extend its service life. The equation of ΔPSI is given by (AASHTO 1993):

$$\Delta PSI = \Delta\, PSI_{traffic} - \Delta\, PSI_{SW\,FH}$$

(2)

In Which:
$\Delta PSI_{traffic}$ = serviceability loss due to traffic load
$\Delta PSI_{SW\,FH}$ = serviceability loss due to swelling (effect of moisture and frost)

### *2.2. Remaining Service Life of Flexible Pavements*

Remaining service life (RSL) is defined as the estimation of pavement service ages remain or the predicted time of pavement serviceability before rehabilitation (Gedafa 2008). The design of pavement service life is recommended for 20 years may be applied to a national highway. Rehabilitation work is needed to restore the pavement performance back to its original condition, wherein the decrease in pavement serviceability index (ΔPSI) will be affected by traffic loads as illustrated in Figure 1.

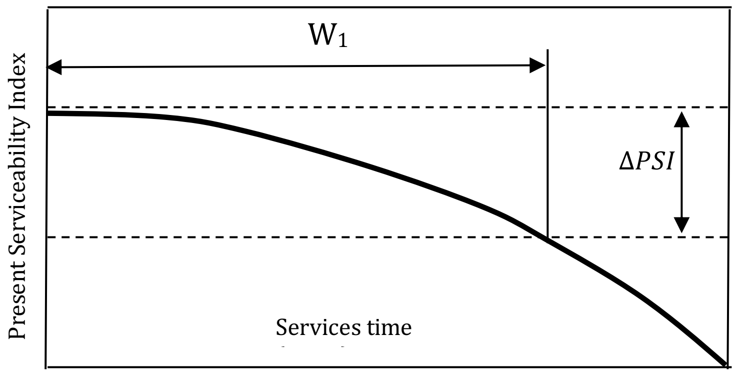


Figure 1: Pavement performance curve (Abaza, 2004)

The assessment of the design period is essential to be applied as a determination of the structural capacity of existing pavements and assists the decision-making process of road maintenance programs for optimizing funds allocation.

## 3. Method

After toll road is operated, the composition and characteristics of traffic using national highway will also change. The idea is to determine and compare the traffic data to evaluate the Equivalent Single Axle Load (ESAL) and then further analyzed for pavement remaining life.
The wider benefit quantified in this study is estimating the impact of diverted traffic on the remaining service life of national highway pavement. The remaining pavement ages period estimation is performed for two scenarios, specifically with and without the toll road operated.

### *3.1. Traffic Estimation*

For estimating the cumulative traffic estimated to use the pavement over the design period, it is necessary to estimate the traffic on national highways and toll roads. The impact of the traffic load for each scenario is obtained by summing the multiplication of three parameters, i.e., average daily traffic, axle load equivalency factor or vehicle damage factor, and annual traffic growth rate for each type of axle load. The formulation of cumulative traffic load is illustrated as mentioned below (AASHTO 1993):

$$\overline{W_{18}} = \sum_i (ADT_i \ x \ E_i x \ G_{Ri}) x \ 365$$

(3)

$$G_{Ri} = \frac{(1 + g_i)^n - 1}{g_i}$$

(4)

Where:
$W_{18}$ = cumulative standard single axle loads for two ways (ESALs)
$ADT_i$ = average daily traffic for axle load i
$E_i$ = axle load equivalent factor (or vehicle damage factor) for axle load i
$g_i$ = traffic growth for vehicle I (%)
n = service life (year)
Traffic growth rates can be estimated by identifying the past trends of traffic growth, and the traffic estimation in the future or at the end of design period ($W_{18}$) is illustrated as mentioned below:

$$W_{18} = D_D \; x \; D_L \; x \; \overline{W}_{18}$$
(5)

Where:
$W_{18}$ = cumulative standard single axle load on design lane (ESAL)
$D_D$ = direction distribution factor
$D_L$ = lane distribution factor
The direction distribution factor ($D_D$) was determined to be 0.5 as the national road are two-way roads and the lane distribution factor ($D_L$) was assumed to be 0.75 as the section considered as undivided roads with two-lane carriage.

*3.2. Pavement Remaining Life*

A second method for calculating the remaining service life in this paper is applying a model to estimate the impact of traffic loads on pavement structure by calculating the service life of pavement. AASTHO 1993 recommended equation to count remaining service life obtained from fatigue equation ($N_p$) and rutting ($N_{1.5}$), therefore could be estimated using the following equation:

$$RL = \left[1 - \left(\frac{N_P}{N_{1.5}}\right)\right] x \; 100\%$$
(6)

With:
RL = Remaining Life (%)
$N_P$ = Total traffic to date
$N_{1.5}$ = Total traffic to pavement failure

**4. Results and Analysis**

*4.1. Medan-Binjai Toll road*

Medan-Binjai Toll Road is a toll road that connects two cities in North Sumatra, mainly Medan and Binjai. The toll road is part of the Trans Sumatra Toll Road with a total length of 16.8 kilometers. Construction of new toll roads can have a positive direct impact by reducing the vehicle operating cost and will significantly reduce vehicle traffic and congestion problems on national road.

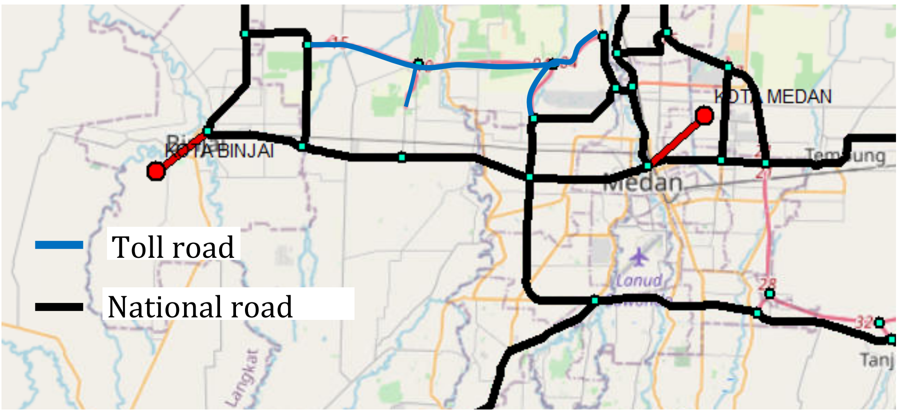


Figure 2: Medan-Binjai Toll Road

Traffic congestion is one of major problems and increases the cost, the delays and more fuel consumed (Lozano, 2014). The evidence indicates that the toll road reduces congestion and increases driving speed on the national road. Traffic diversion is substantially related to toll rate and the elasticity becomes increasingly negative with higher toll fares. Annual Average Daily Traffic (AADT) is a basic measurement that indicates vehicle traffic load on a road segment. The table below illustrates a comparison of empirical AADT data between a national road and a toll road.

*4.2. Diverted traffic*

The empirical data acquired indicates that by diverting a portion of the traffic volume from the national road to the new built-toll road, it is expected that congestion on the national road will be alleviated. As for the effect of toll road, the traffic volume indicates the past trend of the traffic after/before Medan-Binjai toll road operated in 2017, as illustrated in table 1.

Table 1: Traffic volume on Medan-Binjai section

| NO | Vehicle Classification | National Road | | | | | Toll Road | | | | |
|---|---|---|---|---|---|---|---|---|---|---|---|
| | | 2016 | 2017 | 2018 | 2019 | 2020 | 2016 | 2017 | 2018 | 2019 | 2020 |
| 1 | Passenger car | 14.980 | 8.978 | 8.283 | 3.944 | 4.574 | - | 7.226 | 9.245 | 14.889 | 14.450 |
| 5 | Bus | 696 | 399 | 384 | 217 | 331 | - | 335 | 429 | 690 | 670 |
| 7 | single unit 2-axles truck | 4.403 | 3.670 | 3.782 | 3.424 | 3.480 | - | 1.109 | 1.157 | 1.824 | 1.998 |
| 9 | single unit 3-axles truck | 2.249 | 2.091 | 2.207 | 1.978 | 1.981 | - | 533 | 526 | 835 | 1.049 |
| 10 | Single trailer 4 or more-axles | 508 | 377 | 363 | 266 | 255 | - | 137 | 119 | 235 | 263 |

*4.3. The Impact of shifting Traffic on the Performance of National Road Pavements*

Direct effects of investments on toll roads, such as the redistribution of traffic and congestion effects are directly related to the toll road which is under operation. This paper has developed a practical approach for estimating the impact of a toll road on national road performance that has evaluated the pavement remaining life, based on traffic data on Medan-Binjai which was obtained during 2016-2020 period.

The cumulative calculation of ESAL (CESAL) from 2016 to 2020 period is required to estimate the remaining pavement performance ages of the national highway. The CESAL value is to make a comparison between the two scenarios, as illustrated in Fig 3.

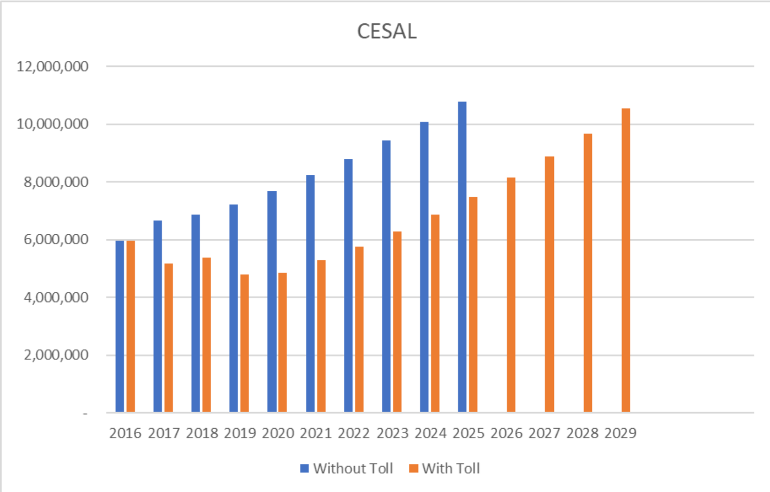


Figure 3: CESAL comparison

The design life of the pavement in this study is 10 years. From the result, we can determine that there is an extension in service life for approximately 6 years from the initial design.

## 5. Discussion

The study did not examine directly the direct impact but the results suggested that the imposing tolls would increase the remaining service life of the national road performance by pushing truck traffic into toll roads that have been designed to handle heavy truck traffic. The development of toll roads does not actually reduce congestion, when the government imposes a high tariff, people will do everything possible to avoid paying it.

This paper examined the broader impact of toll road investment based on national road pavement performance especially on service life remaining. This diversion may not have an increased cost for truckers but this has significant policy implications. At what tariff do truckers divert from national road to the toll road.

This study has implications for the stakeholders involved in the development of Indonesian road infrastructure by highlighting the broader benefit received by the national highway in which the toll road investment occurs.

On encountering the declining road performance and capacity of rehabilitation budgets, the national road authority needs to optimize the allocation of a limited budget. The routine maintenance costs prediction model is needed to examine in future research, and it is important to evaluate the validity of the remaining service period of the pavement by using the International Roughness Index (IRI) value.

## Acknowledgments

This work was supported by Ministry of Research and Technology, DRPM of the year 2020.

## References

Abaza, Khaled A. (2004). *Deterministic performance prediction model for rehabilitation and management of flexible pavement*. The International Journal of Pavement Engineering, 5 (2), https://doi.org/10.1080/10298430412331286977.

American Association of State Highway and Transportation Officials (1993). *AASHTO Guide for design of pavement structures*.

Gedafa, D. S. (2008). *Estimation of remaining service life of flexible pavements from surface deflections*. Kansas state university, Manhattan, KS.

Hajj, E., L. Loria, and P. Sebaaly (2010). *Performance evaluation of asphalt pavement preservation activities*. Transportation Research Record: Journal of the Transportation Research Board, https://doi.org/10.3141%2F2150-05.

Hamdi, Sigit, P. Hadiwardoyo, Correia, A. Gomes, and Pereira, Paulo, (2015). *Road deterioration analysis for the national roads of Indonesia*. [Paper presentation].the 14th International Conference on QIR (Quality in Research), Lombok.

Kaare, K. K. and Koppel, O. (2012). *Performance indicators to support evaluation of road investments. Journal of Economic Literature*, https://doi.org/10.15157/tpep.v20i2.832.

Lozano, Angélica, Granados, Francisco, Guzmán, Alejandro, (2014). *Impacts of modifications on urban road infrastructure and traffic management: a case study*. Procedia - Social and Behavioral Sciences, https://doi.org/10.1016/j.sbspro.2014.12.218.

Lubis, HA, Isnaeni, Muhamad, Sjafruddin, Ade, Dharmowijoyo, Dimas, B. (2005). *Multimodal transport in Indonesia: recent profile and strategy development*, [Paper presentation] The Eastern Asia Society for Transportation Studies, Vietnam.

Mohmand, Yasir, Tariq, Wang, Aihu, Saeed, Abubakr (2016). *The impact of transportation infrastructure on economic growth: empirical evidence from Pakistan*. Transportation Letters: The International Journal of Transportation Research, https://doi.org/10.1080/19427867.2016.1165463.

Singh, Y. Kumar, and Ray, D. S. (2019). *Evaluation of vehicle damage factor in overloading for different types of loading*, International Journal of Engineering Science and Computing.

Syafriana, Saleh Sofyan, M., Anggraini, Renni (2015). *Evaluasi umur layan Jalan Dengan memperhitungkan beban berlebih di ruas jalan lintas timur Provinsi Aceh*, Jurnal Transportasi, 15 (2): https://doi.org/10.26593/jtrans.v15i2.1729.%25p.

World Bank (2013). *State of Logistic Indonesia*.

Yang, Yong-honga, Jiang, Yuan-haob, Wang, Xuan-cang (2016). *Pavement performance prediction methods and maintenance cost based on the structure load*. Procedia Engineering, 137, https://doi.org/10.1016/j.proeng.2016.01.232.